Eur. Phys. J. B **26**, 29–34 (2002)
DOI: 10.1140/epjb/e20020062

THE EUROPEAN PHYSICAL JOURNAL B
EDP Sciences

X-ray scattering study of the phase transitions in crystalline fullerene-biphenyl $C_{60}[(C_6H_5)_2]$

A. Marucci[1], P. Launois[1,a], R. Moret[1], and A. Pénicaud[2]

[1] Laboratoire de Physique des Solides[b], bâtiment 510, Université Paris-Sud, 91405 Orsay, France
[2] Centre de Recherche Paul Pascal, Université de Bordeaux I, avenue Schweitzer, 33600 Pessac, France

Received 31 August 2001 and Received in final form 4 December 2001

Abstract. The phase diagram of the newly synthesized mixed crystal C_{60}-biphenyl is investigated as a function of temperature by single-crystal X-ray scattering. Diffuse scattering investigations evidencing complex disorder and local order effects are presented. Two phase transitions leading to two different doublings of the high temperature unit cell are observed, at 212 K and 147 K. The first transition is attributed to the ordering of twisted biphenyls, which couples to the orientational ordering of the C_{60} molecules as the temperature decreases. Full ordering of the C_{60} molecules is achieved below 100 K only, in the low temperature phase. The rich phase diagram of C_{60}-biphenyl is due to the interplay between fullerene and biphenyl ordering phenomena.

PACS. 61.10.Eq X-ray scattering (including small-angle scattering) – 61.10.Nz Single-crystal and powder diffraction – 61.48.+c Fullerenes and fullerene-related materials – 64.70.Kb Solid-solid transitions

1 Introduction

In the last few years much attention has been focused on the study of the physical properties of fullerene materials, and in particular on the investigation of the electronic properties (conductivity and superconductivity) of fullerene salts prepared by doping fullerene crystals with alkali metals [1]. Further advances may be expected to come from preparative chemistry through the synthesis of different fullerene salts [1–3]. The strategy of preparing new compounds constituted by fullerenes and a different species, and to subsequently dope them with alkali metals, looks very promising for obtaining materials with potentially attractive electronic properties. Neutral mixed fullerene-biphenyl crystals $C_{60}[(C_6H_5)_2]$ have been recently synthesized in this perspective [4]. This article deals with the structural properties of the neutral compound.

Although a significant number of neutral mixed compounds of C_{60} has been reported in literature (a non-exhaustive list of references can be found for example in references [2,5]), detailed structural investigations are rare. In particular the potential orientational degree of freedom linked to the specific shape of the fullerene molecule has received little attention so far. A few notable exceptions, where orientational disorder has been recognized and/or analyzed, are the cases of $C_{60}(C_6H_6)_4$ [6–8], $C_{60}(P_4)_2$ [9] and the molecular complex of hydroquinone and C_{60} [10]. Additionally, although orientationally ordered, the C_{60} molecules present strong uniaxial librational motion in C_{60}(BEDT-TTF)$_2$ (BEDT-TTF= bisethylenedithiotetarthiafulvalene) [11] and C_{60} (bis-BEDT-TTF)CS_2 [12]. In none of the above mentioned examples, has any attempt to analyze orientational disorder by X-ray diffuse scattering been made. Indeed, up to now, pristine C_{60} and C_{70} remain the only fullerene materials on which a thorough analysis of disorder, either static or dynamic, has been performed [13–15].

The structure of the fullerene-biphenyl crystal at room temperature and at 155 K has been refined by Pénicaud *et al.* [4] using four-circle X-ray diffraction data. The results show that the structure is monoclinic at both temperatures, with a doubling of the value of the parameter c at 155 K (room temperature parameters are: $a = 10.424$ Å, $b = 16.932$ Å, $c = 10.32$ Å, $\beta = 100.8°$). The space groups at room temperature and at 155 K are C2/m and I2/a, respectively. The structure of the crystal can be visualized as an alternation of fullerene planes with biphenyl planes, both with nearly hexagonal packing, along the direction **c** (see Fig. 1a). Fullerene-fullerene distances in the (**a**, **b**) plane are d = 9.94 Å and 10.42 Å, to be compared to 10 Å in pure C_{60}. Tetrahedral empty sites, delimited by a triangle of C_{60} and by the hydrogen in meta position of the biphenyl behind or facing the triangle are present, and their size, comparable to that of the empty

[a] e-mail: launois@lps.u-psud.fr
[b] UMR CNRS 8502

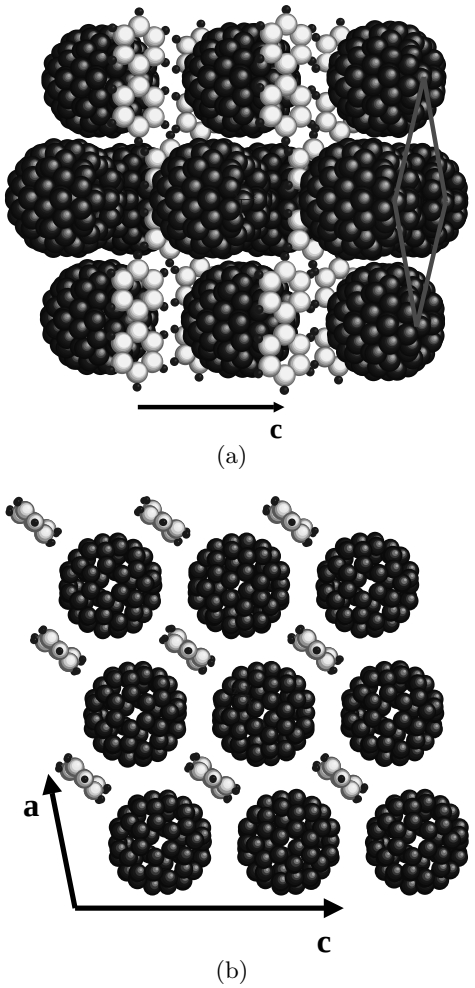

Fig. 1. Representation of the C_{60}-biphenyl crystal structure according to the data in reference [4]: (a) at room temperature, where two C_{60} orientations are superimposed; (b) an (**a**, **c**) layer at 155 K, showing the doubling of the period along c. Figure 1a shows that fullerene (**a**, **b**) planes and biphenyl (**a**, **b**) planes alternate along the direction **c**. The rhomb points to nearly hexagonal packing in the (**a**, **b**) planes.

sites in pure C_{60}, is suitable for doping. At room temperature, the C_{60} molecules are found to adopt two orientations, randomly distributed, while the biphenyl molecule is flat. At 155 K, on the contrary, the two orientations of the fullerenes are found to be ordered (they alternate along **c**; Fig. 1b). Moreover, the biphenyl molecule is twisted with an angle of $\sim$22.9° between the two phenyl rings. The biphenyl molecules exhibit two orientations, corresponding to opposite twist angles and alternating along **c**.

In this article, we will present and discuss new X-ray scattering results, obtained as a function of temperature, to determine the phase diagram of fullerene-biphenyl and the order/disorder phenomena in this crystalline compound. Let us mention that a detailed knowledge of the structural properties of the neutral compound should be useful to better control the alkali metal doping which is under way [4].

2 Experimental results: X-ray diffraction and diffuse scattering

The fullerene-biphenyl crystals have been prepared by slow co-crystallization of a saturated solution of C_{60} and biphenyl in toluene at room temperature [4]. The size of the crystal used for the present study is $0.1 \times 0.2 \times 0.5$ mm^3. Different X-ray scattering investigation methods have been used: (i) the precession technique, to obtain undistorted patterns of selected reciprocal planes at room temperature, (ii) the fixed-crystal fixed-film technique under vacuum and using a cryocooler, to follow the evolution with temperature of both the Bragg peaks and the diffuse scattering, (iii) measurements on a three-circle diffractometer (lifting-detector geometry) equipped with a cryocooler, to obtain quantitative data for the Bragg peak intensities. CuKα or MoKα radiations (corresponding to wavelengths $\lambda = 1.5418$ Å and 0.711 Å, respectively) were selected by reflection on doubly-bent graphite monochromators. Diffraction patterns, taken with techniques (i) and (ii), were recorded with X-ray films or imaging plates.

The C_{60}-biphenyl crystal was first characterized at room temperature using the precession technique. The analysis of precession photographs for different reciprocal layers reveals that the intensity of the Bragg reflections is in good agreement with that calculated using the structural model of reference [4]. These photographs also exhibit diffuse scattering features such as sharp streaks parallel to **b*** and broad planes characterized by $h \pm l = n$ (integer).

Figure 2a shows a photograph taken at room temperature using the Laue monochromatic technique with $\lambda = 0.711$ Å which gives access to large wave-vectors. Two intense diffuse halos at $Q \sim 0.52$ Å^{-1} and $Q \sim 0.84$ Å^{-1} are observed. These halos are typical of strong orientational disorder of C_{60} molecules, as will be discussed in Section 3. Other scattering features are also visible in Figure 2a (modulations of the diffuse intensity inside the halos and some diffuse scattering outside the halos) and they will be discussed in Section 3 as well.

Let us now consider the evolution of the scattering features that occurs upon lowering the temperature.

Diffraction patterns obtained at room temperature and at $T = 200$ K are shown in Figures 3a and b. It can be seen that superstructure Bragg peaks are present at $T = 200$ K. Simulations of the diffraction pattern allowed us to index these superstructure peaks: their indices are $(h, k, l + 1/2)$ when referred to the high temperature reciprocal lattice (h, k and l being integer). Moreover, they satisfy the condition $h + k + 2l = 2n$ in agreement with what is expected for the body-centered monoclinic space group I2/a and for the doubling of the parameter c, as determined in reference [4] at 155 K. These results show evidence that the structural transition between the two monoclinic phases C2/m and I2/a observed at room temperature and 155 K, respectively, as reported in reference [4], actually occurs above 200 K.

The intensities of the superstructure Bragg peaks have been measured as a function of temperature using

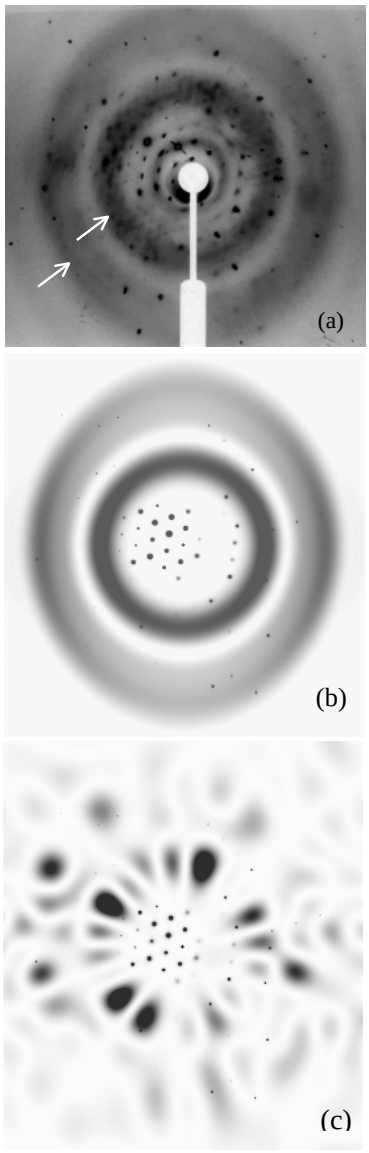

Fig. 2. (a) Fixed-crystal fixed-film photograph at room temperature (MoKα radiation, $\lambda = 0.711$ Å, cylindrical film of diameter $\Phi = 57.3$ mm), the crystal is mounted with (**a**+**b**) approximately vertical perpendicular to the X-ray beam, (b) simulation of the diffuse scattering for complete orientational disorder of the C_{60} molecules, (c) simulation of the diffuse scattering for the C_{60} disorder proposed in reference [4], with two C_{60} orientations. In (a), the arrows point toward diffuse halos at $Q \sim 0.52$ Å^{-1} and 0.84 Å^{-1} (Q is defined by $Q = 2\sin(\theta)/\lambda$).

a three-circle diffractometer. As a typical example, the variation of the intensity of the superstructure peak (2, 9, −1.5) in the range 170−250 K is displayed in Figure 4. It shows that the transition between the monoclinic phases C2/m (phase I) and I2/a (phase II) occurs at $T_{C1} \sim 212$ K and that it is of second order. Pretransitional diffuse scattering peaks are observed above T_{C1}. They have been analyzed with Ornstein-Zernicke Lorentzian correlation functions along the directions **a***, **b*** and **c***.

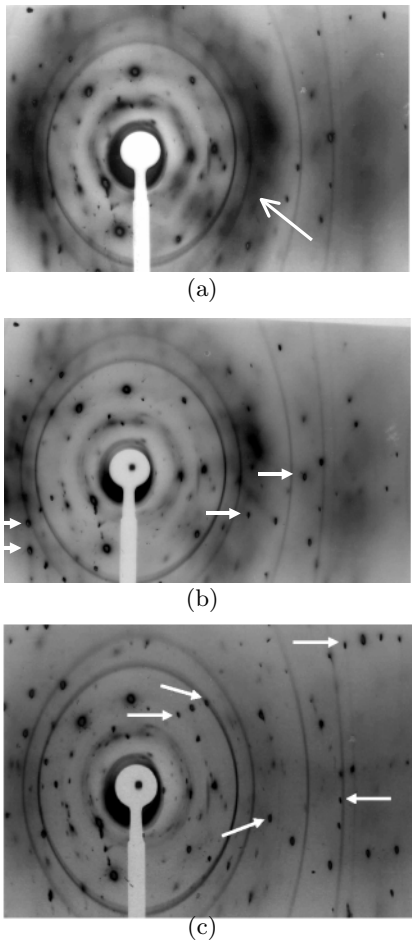

Fig. 3. Fixed-crystal fixed-film photographs taken at: (a) room temperature, (b) $T = 200$ K, (c) $T = 100$ K (CuKα radiation, $\lambda = 1.5418$ Å, cylindrical film $\Phi = 61$ mm). The crystal is mounted with (−**a**+4**c**) approximately vertical. The arrow in (a) points toward the $Q \sim 0.52$ Å^{-1} diffuse halo. The arrows in (b) point toward superstructure peaks corresponding to a doubling of the parameter c. Those in (c) point toward superstructure peaks corresponding to the unit cell (**a** + **b**, **a**−**b**, **c**). The sharp rings are due to diffraction from the sample holder.

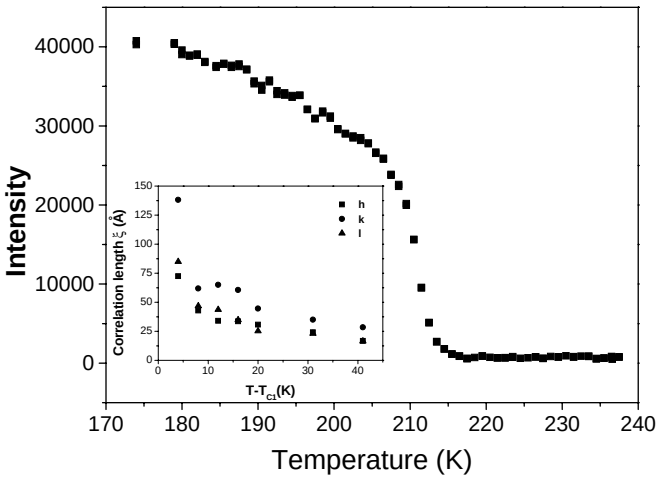

Fig. 4. Temperature dependence of the intensity and correlation lengths along **a**, **b** and **c** (inset) for the (2, 9, −1.5) superstructure reflection.

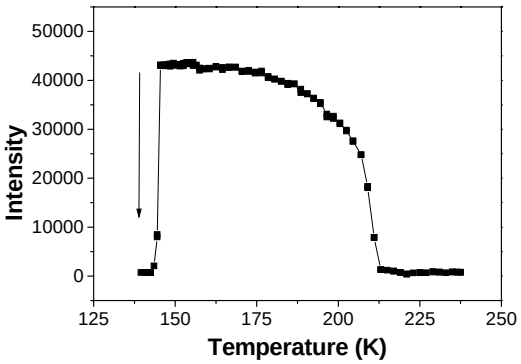

Fig. 5. Temperature dependence of the intensity of superstructure peaks of phases II and III: (a) (2, 9, −1.5) and (b) (1.5, 8.5, −1).

The correlation lengths thus obtained are shown as a function of temperature in the inset of Figure 4.

The comparison of the diffraction patterns at T = 200 K (Fig. 3b) and at 100 K (Fig. 3c) shows that another phase transition occurs between 200 K and 100 K. The superstructure peaks (h, k, $l + 1/2$) disappear while new peaks around ($h + 1/2$, $k + 1/2$, l), as indexed in the high temperature phase structural basis, appear. The corresponding low temperature phase, evidenced here for the first time, is named phase III.

Detailed three-circle experiments allowed us to show that phase III has a triclinic symmetry, and that two types of domains of phase III are present in the crystal, because of the symmetry lowering from monoclinic to triclinic. Refinement of peak positions within one domain of phase III leads to unit cell angles β and γ which are almost the same as for the high temperature phases (100.8° and 90°, respectively), while the angle α, between the axis **b** and **c**, is found to be 90.9°, instead of 90°. Moreover the analysis of the orientational relationships between the domains shows that the deviation of α from 90° mainly corresponds to a change in the orientation of the axis **c**, while the planes (**a**, **b**) are unchanged. Superstructure peaks at ($h + 1/2$, $k + 1/2$, l) correspond to a unit cell defined by the vectors (**a**+**b**, **a**−**b**, **c**). The evolution of the intensities of the superstructure peak (2, 9, −1.5), characteristic of phase II, and of the (1.5, 8.5, −1) peak characteristic of phase III, is displayed in Figure 5. The transition between phases II and III is found to occur at $T_{C2} \sim 147$ K and to be first order with an hysteresis of about 4 K.

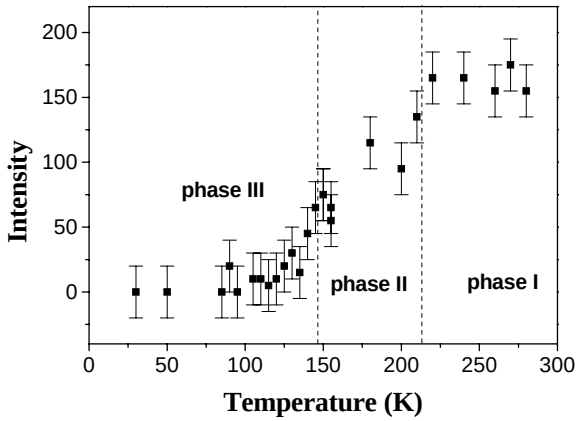

Fig. 6. Intensity of the first diffuse scattering halo ($Q \sim 0.52$ Å^{-1}) *versus* temperature.

The evolution of the diffuse scattering halos with temperature is revealed in Figures 3a–c. The diffuse scattering intensity is quite strong at room temperature, decreases at 200 K and becomes negligible at 100 K. This evolution has been followed quantitatively using measurements made with the imaging plate and diffractometer techniques, both techniques providing similar results (Fig. 6). The intensity of the diffuse scattering halos is found to be nearly constant in phase I. Below the second order transition at ∼212 K, it starts decreasing until ∼100 K, where it disappears completely.

3 Discussion

The discussion is organized as follows. The structural relations between phases I, II and III are discussed first. Then we consider the complex diffuse scattering features measured at room temperature. The evolution of the diffuse halos with temperature is finally presented with a possible scenario for the ordering phenomena as a function of temperature.

The unit cells in phases I, II and III are (**a**, **b**, **c**), (**a**, **b**, 2**c**) and (**a**+**b**, **a**−**b**, **c**), respectively. Surprisingly, the superstructure peaks characteristic of phase II disappear in phase III. Both phases II and III correspond to different doublings of the phase I unit cell, a rather unusual feature. Furthermore, the transition towards phase III corresponds to a symmetry lowering with a change of the angle α from 90° to ∼90.9°, due to a small reorientation of the axis **c**. The tilt of the **c** axis is probably induced by the complex interactions which govern the stacking of the alternating dense (**a**, **b**) layers of fullerenes and byphenyl molecules. Finally, let us notice that the transition between phases II and III is first order, as expected between two phases with no group to sub-group relation.

The room temperature diffuse scattering is complex and composed of several components, which are recalled

and discussed below: i) pretransitional diffuse peaks at $(h,\ k,\ l+1/2)$, ii) lines along **b***, iii) (hkl) planes with $h \pm l =$ integer, iv) broad diffuse halos at wave vectors $Q \sim 0.52$ Å^{-1} and $Q \sim 0.84$ Å^{-1}.

As shown in Figure 4, the $(h,\ k,\ l+1/2)$ diffuse peaks are due to pretransitional diffuse scattering. Correlation lengths along directions **a**, **b** and **c** increase when lowering temperature in phase I (see inset). The transition from phase I towards phase II appears rather isotropic as the correlation lengths are of the same order of magnitude.

The sharp diffuse lines along **b*** are associated to stacking faults between (**a**, **c**) planes. The broad diffuse planes with $h \pm l =$ integer correspond to some kind of disordered "chains" running along [1,0,±1] directions, where there is an alternation between biphenyl and fullerene molecules, as shown in Figure 1b. The correlation length along the chains, deduced from fitting the intensity lineshape across the planes with a Lorentzian, is about 50 Å. The nature of these stacking faults and of these "chains" would be interesting to clarify because it is probably related to the interactions between the biphenyl and fullerene molecules.

Let us now discuss in more details the diffuse scattering halos observed at room temperature. We have considered two different models with full and partial orientational disorder and the corresponding simulated diffuse scattering patterns are shown in Figure 2b and c, respectively.

The simulation in Figure 2b was performed assuming that the C_{60} molecules can exhibit any orientation, with equal probability, and that the relative orientations of neighboring molecules are not correlated. The diffuse scattering intensity was calculated from [16,17]:

$$I_D(\mathbf{Q}) \propto f_C(Q)^2 \sum_{l \neq 0} [g_l j_l(2\pi QR)]^2 \qquad (1)$$

where Q is the modulus of the wave vector $\mathbf{Q}$, f_C is the carbon form factor, g_l is the C_{60} molecular form factor for the l value of angular momentum, calculated within the symmetry-adapted functions formalism [18], the functions j_l are spherical Bessel functions and R is the radius of the C_{60} molecule.

In Figure 2c, the simulation was performed for two differently oriented molecules randomly distributed on lattice sites. We have chosen the orientations deduced from the structural analysis of reference [4]. As demonstrated in reference [19], in such a case, the diffuse intensity reads:

$$I_D(\mathbf{Q}) \propto \mid F_1(\mathbf{Q}) - F_2(\mathbf{Q}) \mid^2 \qquad (2)$$

where $F_1(\mathbf{Q})$ and $F_2(\mathbf{Q})$ are the form factor of the C_{60} molecule in its two orientations. The lack of agreement between Figure 2a and c rules out the second model of orientational disorder with two orientations for the C_{60} molecules at room temperature. A much better agreement is found between Figure 2a and b, which shows that the fullerene molecules exhibit strong orientational disorder with nearly all possible orientations at room temperature [20]. Nevertheless, the presence of intensity modulations of the diffuse scattering halos, which take place inside the Brillouin zone, indicates that some orientational correlations between the C_{60} molecules are present; their analysis is not pursued here. Modulations of this type have, for instance, been observed in pure C_{60} [17,21,25] and allowed one to test different models of intermolecular interactions [13,22–25] and to determine intermolecular orientational pair correlation functions [13,15].

The variation of the intensity of the first diffuse halo as a function of temperature is shown in Figure 6. The intensity is roughly constant in phase I. It starts to decrease below 212 K in phase II, and it vanishes at ∼100 K, in phase III. We can thus assert that the orientational disorder of the C_{60} molecules is unchanged with temperature in phase I, while in phase II there is a progressive improvement of the C_{60} orientational order. At 155 K, the diffuse scattering intensity is only 35% of the high temperature value: roughly 65% of the molecules are now orientationally ordered. The structural analysis performed at 155 K in reference [4] shows that these C_{60} molecules are ordered with two preferential orientations alternated along the direction **c** (as shown in Fig. 1b). The reason why the ordering of C_{60} occurs only progressively as a function of temperature is still an open question.

Combining the results obtained in this article with the structural refinements of reference [4], we can draw a schematic picture of ordering phenomena in C_{60}-biphenyl as a function of temperature. At room temperature, strong disorder is present, with, in particular, complete C_{60} orientational disorder that makes all the fullerenes equivalent in phase I. The biphenyl molecules are, on average, flat. The structure I2/a, determined for phase II at 155 K [4], corresponds to the ordering of twisted biphenyl molecules and of fullerenes with two orientations alternated along the direction **c**. Our results on the progressive ordering of fullerenes as a function of temperature in phase II, infer that the transition between phase I and phase II at 212 K is in fact driven by the ordering of twisted biphenyl molecules only. This ordering is indeed sufficient to satisfy doubling of the unit cell along **c** and the I2/a space group symmetry requirements. The C_{60} ordering starts at ∼212 K, after the second order phase transition, in a compatible way with the I2/a symmetry. The C_{60} orientational ordering is not complete at the transition to phase III (147 K) and it proceeds in this phase until completion at about 100 K. However, the superstructures and symmetries of phases II and III are different, which implies that a full re-ordering of both biphenyl and the already ordered C_{60} molecules occurs at the transition between these two phases.

In brief, the phase diagram of C_{60}-biphenyl is very rich due to the combined ordering phenomena of its two different molecular constituents. Concerning the progressive ordering of the C_{60} molecules, some similarity may be noticed between C_{60}-biphenyl and pure C_{60}, as follows. In the low temperature phase $Pa\overline{3}$ of pure C_{60}, the C_{60} molecules can take two sorts of orientations, orientation 'P', with pentagons looking towards the double-bond of neighboring molecules, and orientation 'H', with hexagons facing these double-bonds [26]. The diffuse

scattering disorder due to the existence of these two orientations diminishes with temperature, while more and more molecules get 'P' orientations [27,28].

4 Conclusion

In this work, we have performed a study of the phase diagram of fullerene-biphenyl $C_{60}[(C_6H_5)_2]$ as a function of temperature. The fullerene-biphenyl phase diagram is very rich due to the interplay between fullerene and biphenyl ordering processes. The results show that it is more complex than indicated by previous four-circle measurements, where two different monoclinic phases (phases I and II) were evidenced at room temperature and 155 K [4]. In particular, our results show the existence of a third phase (phase III), observed below ∼147 K.

The transition between phases I and II is shown to occur at 212 K and to be second order. Phase II is characterized by a doubling of the unit cell of phase I, due to the doubling of the parameter *c*. Phase III is triclinic and it corresponds to a different sort of doubling of the phase I unit cell, with parameters (**a**+**b**, **a**−**b**, **c**). These different unit cell doublings in phases II and III are unusual. The transition between phases II and III occurs at ∼147 K and is first order with hysteresis. The original phase diagram of C_{60}-biphenyl would be worth studying in more details. In particular, the effect of pressure would be interesting to measure. Pressure may stabilize one of the low temperature phases with respect to the other and, for instance, lead to the suppression of the intermediate phase II with a direct transition between phases I and III.

Several diffuse scattering features have been measured at room temperature, evidencing complex disorder or local order phenomena. In particular strong diffuse halos are an evidence of C_{60} orientational disorder. These molecules start to get orientationally ordered below the transition at 212 K, but they actually get completely ordered only in phase III at ∼100 K.

A.M. thanks the European Union Research Network FULPROP and the Centre National de la Recherche Scientifique (CNRS) in France for an Associated Scientist position. A.P. acknowledges support from Conseil Régional d'Aquitaine. We thank Giampiero Ruani and Dimitri Pallés for helpful discussions and Olinda Carreón for single crystal growing.

References

1. M.J. Rosseinsky, Chem. Mater. **10**, 2665 (1998).
2. A. Pénicaud, Fuller. Sci. Technol. **6**, 731 (1998).
3. C.A. Reed, R.D. Bolskar, Chem. Rev. **100**, 1075 (2000).
4. A. Pénicaud, O.Y. Carreón, A. Perrier, D.J. Watkin, C. Coulon, J. Mater. Chem. to appear (2002).
5. M.S. Dresselhaus, G. Dresselhaus, P. Eklund, *Science of Fullerenes and Carbon Nanotubes* (Academic Press 1996).
6. M.F. Meidine, P.B. Hitchcock, H.W. Kroto, R. Taylor, D.R.M. Walton, J. Chem. Soc., Chem. Commun., 1534 (1992).
7. A.L. Balch, J.W. Lee, B.C. Noll, M.M. Olmstead, J. Chem. Soc., Chem. Commun., 56 (1993).
8. H.B. Bürgi, R. Restori, D. Schwarzenbach, A.L. Balch, J.W. Lee, B.C. Noll, M.M. Olmstead, Chem. Mater. **6**, 1325 (1994).
9. I.W. Locke, A.D. Darwish, H.W. Kroto, K. Prassides, R. Taylor, D.R.M. Walton, Chem. Phys. Lett. **225**, 186 (1994).
10. O. Ermer, Helv. Chim. Acta **74**, 1339 (1991).
11. A. Izuoka, T. Tachikawa, T. Sugawara, Y. Suzuki, M. Konno, Y. Saito, H. Shinohara, J. Chem. Soc., Chem. Commun., 1472 (1992).
12. A. Izuoka, T. Tachikawa, T. Sugawara, Y. Saito, H. Shinohara, Chem. Lett., 1049 (1992).
13. P. Launois, S. Ravy, R. Moret, Int. J. Mod. Phys. B **13**, 253 (1999).
14. P. Launois, R. Moret, J. Phys. IV **10**, 193 (2000).
15. S.L. Chaplot, L. Pintschovius, Int. J. Mod. Phys. B **13**, 217 (1999).
16. J.D. Axe, S.C. Moss, D.A. Neumann, in *Solid State Physics: Advances in Research and Applications*, edited by H.E. Ehrenreich, F. Spaepen (Academic Press, New York, 1994), Vol. 48, pp. 149–224.
17. P. Launois, S. Ravy, R. Moret, Phys. Rev. B **52**, 5414 (1995).
18. K.H. Michel, J.R.D. Copley, D.A. Neumann, Phys. Rev. Lett. **68**, 2929 (1992).
19. P. Launois, R. Moret, N.R. de Souza, J.A. Azamar-Barrios, A. Pénicaud, Eur. Phys. J. B. **15**, 445 (2000).
20. In agreement with this conclusion, let us mention recent Raman experiments performed at room temperature: under light irradiation, dimers and linear polymers are formed at the surface of the crystal [A. Marucci, P. Launois, R. Moret, D. Pallés, G. Ruani, A. Pénicaud, *Electronic Properties of Novel Materials - Science and Technology of Molecular Nanostructures: XV International Winterschool*, edited by H. Kuzmany *et al.*, AIP Conf. Proc. No 591 (AIP New York, 2002), p. 153. The C_{60} orientational disorder is probably dynamical and the rotation of the C_{60} makes double bonds of neighboring molecules face each other, an important requisite for polymerization.
21. R. Moret, S. Ravy, J.M. Godard, J. Phys. I France **2**, 1699 (1992); **3**, 1085 (1993).
22. S. Ravy, P. Launois, R. Moret, Phys. Rev. B **53**, R10532 (1996); Phys. Rev. B **54**, 17224 (1996).
23. P. Launois, S. Ravy, R. Moret, Phys. Rev. B **55**, 2651 (1997); Phys. Rev. B **56**, 7019 (1997).
24. J.R.D. Copley, K.H. Michel, J. Phys. Cond. Matt. **5**, 4353 (1993); K.H. Michel, J.R.D. Copley, Z. Phys. B **103**, 369 (1997).
25. L. Pintschovius, S.L. Chaplot, G. Roth, G. Heger, Phys. Rev. Lett. **75**, 2843 (1995).
26. W.I.F. David, R.M. Ibberson, T.J.S. Dennis, J.P. Hare, K. Prassides, Europhys. Lett. **18**, 219 (1992); **18**, 735 (1992).
27. S.L. Chaplot, L. Pintschovius, M. Haluska, H. Kuzmany, Phys. Rev. B **51**, 17028 (1995).
28. R. Moret, P. Launois, S. Ravy, M. Julier, J.M. Godard, Synth. Metals **86**, 2327 (1997).